

A Novel Role of AIM2 Inflammasome-Mediated Pyroptosis in Radiofrequency Ablation of Hepatocellular Carcinoma

Wang C, Wang Q and Chen W*

Department of Interventional Radiology, First People's Hospital of Changzhou, The Affiliated Hospital of Suzhou University, China

*Corresponding author:

Wenhua Chen,
Department of Interventional Radiology, First
People's Hospital of Changzhou, The Affiliated
Hospital of Suzhou University, 185 Juqian
St. Changzhou, Jiangsu 213000, China,
E-mail: 937139075@139.com

Received: 20 Dec 2022

Accepted: 23 Jan 2023

Published: 03 Feb 2023

J Short Name: ACMCR

Copyright:

©2023 Chen W. This is an open access article distributed under the terms of the Creative Commons Attribution License, which permits unrestricted use, distribution, and build upon your work non-commercially

Citation:

Chen W, A Novel Role of AIM2 Inflammasome-Mediated Pyroptosis in Radiofrequency Ablation of Hepatocellular Carcinoma. *Ann Clin Med Case Rep.* 2023; V10(11):1-10

Keywords:

Absent in melanoma 2; Hepatocellular carcinoma; Inflammasome; Pyroptosis; Radiofrequency ablation

Abbreviations:

AIM2: Absent in Melanoma 2; ELISA: Enzyme-Linked Immunosorbent Assay; FLICA: Fluorescent-Labeled Inhibitors of Caspase; GAPDH: Glyceraldehyde-3-Phosphate Dehydrogenase; HBV: Hepatitis B Virus; HCC: Hepatocellular Carcinoma; HCV: Hepatitis C Virus; H&E: Hematoxylin and Eosin; IL-1 β : Interleukin-1 β ; IL-18: Interleukin-18; LDH: Lactate Dehydrogenase; NC: Nonspecific Control; qRT-PCR: Quantitative Reverse Transcription-Polymerase Chain Reaction; RFA: Radiofrequency Ablation; SD: Standard Deviation

1. Abstract

Background: Hepatic inflammation and inflammasome-mediated mechanisms are involved in the pathogenesis of Hepatocellular Carcinoma (HCC), and Absent in Melanoma 2 (AIM2) triggers activation of the inflammasome cascade. Until now, it remains unclear whether and how AIM2 plays a role in HCC and Radiofrequency Ablation (RFA). This study aimed to investigate whether RFA induces pyroptosis in HCC through AIM2-inflammasome signaling in vivo and in vitro.

Methods: BALB/c nude mice were used to generate HepG2 or SMMC-7721 cell-derived tumor xenografts. HCC cells with knockout or overexpression of AIM2 were created for functional and mechanistic studies.

Results: We found that RFA significantly suppressed the tumor growth in mice bearing HCC xenografts. Flow cytometry analysis revealed that RFA induced pyroptosis. Furthermore, AIM2, NLRP3, caspase-1, γ -H2AX, and DNA-PKc had significantly greater expression levels in the liver tissues from mice treated with RFA versus those of the controls. In parallel, the expression levels of Interleukin (IL)-1 β and IL-18 were significantly greater in the HepG2 and SMMC-7721 cell-derived xenograft mice treated with

RFA compared to those without receiving RFA. Of note, a greater effect was achieved in the RFA complete ablation group versus the partial ablation group. Moreover, studies in cell lines with knockout or overexpression of AIM2 demonstrated that AIM2 exerted a role in RFA-induced pyroptosis.

Conclusion: The findings of this study indicate that RFA suppresses tumor growth through inducing pyroptosis and that AIM2-mediated pyroptosis is an important cell death mechanism.

Therefore, intervention of AIM2-mediated inflammasome signaling may assist in improving RFA treatment for HCC.

2. Introduction

Hepatocellular Carcinoma (HCC) is among the most common malignancies and a leading cause of cancer-related deaths globally [1]. It has been noted that the majority of HCC cases occur in Asian countries [2]. For instance, in China, the incidence of HCC is considerably high, accounting for approximately 50% of all newly diagnosed HCC cases across the world, and can be attributed to the particularly high prevalence of chronic Hepatitis B Virus (HBV) infection [2-4]. In fact, HBV and Hepatitis C Virus (HCV) are common causes of chronic hepatitis and progressive-

lycauseinflammationoftheliver.Althoughtheexactpathogenic

mechanisms underlying HCC remain to be elucidated, hepatic inflammation and inflammasome-mediated molecular mechanisms have been proposed to play a role in the pathogenesis of HBV- and HCV-related HCC; in addition, HCC is considered an inflammation-related malignancy [5-8]. Of the curative treatments for HCC, Radiofrequency Ablation (RFA) has emerged as an effective and safe treatment for patients with a small-sized tumor, usually 3cm or less in diameter. In comparison with traditional hepatic resection and liver transplantation, RFA has been associated with less invasiveness and a shorter hospital stay. Despite the advantages and increasing application of RFA in the treatment of HCC, the molecular mechanisms underlying the action of RFA are not well understood.

Absent in Melanoma 2 (AIM2) is a cytosolic receptor in the pyrin and HIN domain-containing protein family [9, 10]. AIM2 has been shown to sense and bind to double-stranded DNA and to apoptosis-associated speck-like protein, thus triggering activation of the inflammasome signaling cascade and orchestrating assembly of the AIM2 inflammasome [11-13]. Activation of the AIM2 inflammasome, which consists of multiple proteins, represents one key aspect of the inflammation pathways. The AIM2 inflammasome can activate caspase-1, leading to induction, maturation, and release of key proinflammatory cytokines such as interleukin-1 β (IL-1 β) and interleukin-18 (IL-18) [14]. Therefore, the AIM2 inflammasome possesses both proinflammatory and proapoptotic properties to mediate pyroptosis, which has been implicated in the host defense, thus combating microbial invasion, carcinogenesis, and cancer progression. A number of previous studies have reported that AIM2 expression is decreased in HCC tissues versus histologically normal tissues and that lower levels of AIM2 are significantly correlated with more advanced HCC. Until now, it remains largely unknown whether and how AIM2 plays a role in HCC. In addition, whether and how AIM2 exerts a role in the mechanism of action of RFA for HCC has not yet been explored.

In the present study, we aimed to investigate the roles of AIM2 in HCC and the action of RFA for the treatment of HCC in mice with xenograft tumors as well as in hepatoma cells. The findings obtained through conducting this study may offer a better understanding of the biological function of AIM2, the AIM2 inflammasome, and pyroptosis in HCC, thereby assisting in improving RFA treatment for HCC.

3. Materials and Methods

Experimental Animals

BALB/c nude mice (4–6 weeks old) were purchased from Jiangsu Synthgene Biotechnology Co., Ltd. (Nanjing, Jiangsu, China). The mice were housed under controlled conditions and were allowed tap water ad libitum throughout the period of the animal experiments. To establish the HepG2 and SMMC-7721 cell-derived tumor xenograft animal models, BALB/c nude mice were subcutaneously injected with HepG2 cells (1×10^7 cells suspended in 100

μ L of serum-free RPMI1640 medium) or SMMC-7721 cells (1×10^7 cells suspended in 100 μ L of serum-free RPMI1640 medium). HepG2 or SMMC-7721 cell-derived xenograft nude mice were randomly assigned to receive RFA complete ablation, RFA partial ablation, or no ablation as a control (no ablation). Four weeks following the treatment, the mice were anesthetized and sacrificed by cervical dislocation, and the tumors were collected. The weights and volumes of the excised tumors were analyzed.

The study involving experimental mice was reviewed and approved by the Ethics Committee of Changzhou First People's Hospital (Approval No. 2018-025). All methods were carried out in accordance with the local institutional and national guidelines and regulations. In addition, they were performed in compliance with the international regulations for the use of laboratory animals.

RFA

HepG2 or SMMC-7721 cell-derived xenograft nude mice were treated with RFA using a Cool-tip TMRFA Electrode kit (Covidien Iic, Mansfield, MA, USA), according to the manufacturer's protocol. For the in vitro study, RFA was performed using a thermal needle to treat SMMC-7721 cells.

Histology

Tumor tissues of the HepG2 and SMMC-7721 cell-derived xenograft nude mice were fixed, paraffin-embedded, and cut into 2- μ m-thick sections. After staining with hematoxylin and eosin (H&E), the slides were examined by light microscopy.

Immunohistochemistry

Immunohistochemical analysis was carried out to assess the protein expression of AIM2, NLRP3, and caspase-1 in the liver tissues from HepG2 and SMMC-7721 cell-derived xenograft nude mice treated with or without RFA. The liver tissues were collected, fixed in 10% formalin, and embedded in paraffin. The paraffin sections of the liver tissues were hydrated, and the slides were then incubated with primary antibodies, including those targeting AIM2 (Bioss Antibodies, Beijing, China), NLRP3 (Abcam, Cambridge, UK), and caspase-1 (Abcam, Cambridge, UK), at 4 °C overnight. The resulting slides were then incubated with 3,3'-diaminobenzidine (DAB), a substrate for horseradish peroxidase using a DAB Peroxidase Substrate kit, according to the manufacturer's instructions (Vector Laboratories, Burlingame, CA, USA). Images were taken by an Olympus digital electron microscope (Olympus, Tokyo, Japan). The immunoreactivities of the immunohistochemical images were evaluated for each slide.

Cell Culture

Two human hepatocellular carcinoma cell lines, including HepG2 and SMMC-7721, were obtained from Shanghai Binsui Biotechnology (Shanghai, China) and used for the in vitro studies. The HepG2 and SMMC-7721 cells were cultured in RPMI1640 medium (Hyclone, Marlborough, MA, USA) supplemented with 10% (v/v) fetal bovine serum, 100 μ g/mL streptomycin, and 100 units/

mLpenicillin.

OverexpressionandKnockoutofAIM2

ThepcDNA3.1vectorwasusedtoconstructtheexpressionvector (OS-AIM2)byinsertingthecDNAsequenceencodingAIM2.The successful construction of the expression vector OS-AIM2 was verified by sequencing. SMMC-7721 cells were transfected with OS-AIM2foroverexpressionofAIM2usingLipofectamine2000 Reagent (Invitrogen, Carlsbad, CA, USA). Silencing of AIM2 wasachievedbyCRISPR/Cas-9geneeditingofthe AIMgene in SMMC-7721 cells. SMMC-7721 cells were transfected with CRISPR/Cas-9-AIM2forknockoutofAIM2usingLipofectamine 2000 Reagent (Invitrogen, Carlsbad, CA, USA).

LactateDehydrogenaseReleaseAssay

Cellulardamagewasmeasuredbyalactatedehydrogenase(LDH) release assay in which the LDH levels in the cell culture supernatant of SMMC-7721 cells were determined using an LDH release assaykit(Abcam,Cambridge,UK),accordingtothemanufacturer's instructions.

FlowCytometryAnalysisofPyroptotic Cells

Pyroptosis was measured on a flow cytometer (Becton, Dickinson and Company, Franklin Lakes, NJ, USA). Fluorescent-labeled inhibitors of caspase (FLICA) probe assays (AAT Bioquest, Sunnyvale, CA, USA) were conducted to examine the pyroptosis, according to the manufacturer's instructions. Pyroptotic cells were specifically stained by FAM-FLICA-caspase-1 and propidium iodide staining.

Enzyme-Linked Immunosorbent Assay (ELISA)

ELISA was carried out to determine the serum levels of IL-1 β and IL-18 in HepG2 and SMMC-7721 cell-derived xenograft nude mice treated with or without RFA as well as in the cell culture supernatant of SMMC-7721 cells using ELISA kits (Abcam, Cambridge, UK), according to the manufacturer's instructions.

Real-Time Quantitative Reverse Transcription–Polymerase Chain Reaction (qRT-PCR)

Total RNA was extracted from SMMC-7721 cells using TRIzol (Invitrogen, Waltham, MA, USA). The total RNA samples were transcribed into cDNA, according to the manufacturer's instructions. qRT-PCR was carried out to measure the mRNA expression of target genes (pyroptosis-related genes). The mRNA expression of β -actin was used as an internal control. The relative mRNA levels of target genes were obtained by using the 2 $^{-\Delta\Delta C_t}$ method, with all assays performed in triplicate. Fold-change values were calculated by comparative Ct analysis after normalization to β -actin. The primers used in the qRT-PCR analysis were as follows: AIM2, forward primer: 5'-ATCAGGAGGCTGATCCCAAA-3'; reverse primer: 5'-TCTGTTCAGGCTTAACATGAG-3'; β -actin, forward primer: 5'-GGCACCACCTTCTACAATG-3'; reverse primer: 5'-TAGCACAGCCTGGATAGCAAC-3'.

Western Blot Analysis

Western blot analysis was performed to examine the hepatic protein levels of AIM2 as well as the key inflammasome- and pyroptosis-related proteins, such as NLRP3 (Abcam, Cambridge, UK), caspase-1 (Abcam, Cambridge, UK), γ -H2AX (Abcam, Cambridge, UK), and DNA-PKc (Sangon Biotech, Shanghai, China). The protein expression of glyceraldehyde-3-phosphate dehydrogenase (GAPDH) was used as a loading control. In brief, 30–50 μ g of total protein was separated on 4–15% sodium dodecyl sulfate–polyacrylamide gels. After electrophoretic transfer onto ImmunBlot polyvinylidene difluoride membranes, the resulting membranes were blocked with phosphate-buffered saline containing 5% nonfat dry milk and 0.1% Tween-20, followed by incubation with primary antibody overnight at 4 °C. The membranes were then incubated with secondary antibodies (dilution, 1:10,000) at room temperature for 1 h. An imaging system was used to determine the relative optical density of each specific band in the western blot analysis.

Statistical Analysis

Statistical analysis was conducted with SPSS software version 16.0 for Windows (SPSS, Chicago, IL, USA). All experiments included at least triplicate samples for each treatment group, and data were expressed as the mean \pm Standard Deviation (SD). For the immunohistochemistry and western blot results, representative images are represented. Analysis of Variance (ANOVA) was applied to compare means of multiple groups. $P < 0.05$ indicated a significant difference between groups.

4. Results

RFA Suppressed Tumor Growth in Subcutaneous Xenograft Nude Mice

We initially assessed the effects of RFA on in-vivo tumor growth in subcutaneous xenograft nude mice. As shown in Figure 1A–B, HepG2 and SMMC-7721 cell-derived xenograft tumors grew progressively in the control nude mice without the RFA treatment as a control, whereas RFA treatment markedly suppressed the tumor growth as demonstrated by the significantly smaller tumor size and the lower tumor weight compared with those of the controls after four weeks of treatment. It was also noted that the mean tumor sizes were significantly smaller and the tumor weights were significantly lower in the HepG2 and SMMC-7721 cell-derived xenograft nude mice treated with complete RFA ablation than in those treated with partial RFA ablation after four weeks of treatment ($P < 0.05$) (Figure 1A–B). The results also indicated that the inhibitory effects on the in-vivo tumor growth were greater in the HepG2 and SMMC-7721 cell-derived xenograft nude mice treated with complete RFA than in those treated with partial RFA ablation (Figure 1A–B). Consistent with the changes in the tumor size and weight, H&E staining of tumor sections revealed a significant reduction in the number of tumor cells in the HepG2 and SMMC-7721 cell-derived xenograft nude mice treated with complete or partial RFA

ablation, compared with the control mice (Figure 1C). In addition, flow cytometry analysis showed that the percentages of pyroptotic cells were 12.62%, 10.75%, and 5.49% (HepG2) and 26.42%, 9.84%, and 3.53% (SMMC-7721) in the complete, partial, and no RFA ablation groups, respectively (Figure 1D). Statistical analysis

indicated that the proportion of pyroptotic cells was significantly increased in the tumor cells of the subcutaneous xenograft nude mice treated with RFA partial or complete ablation, compared with no RFA ablation as a control ($P < 0.01$) (Figure 1D). Moreover, there was a significantly greater effect in the RFA complete ablation group compared with the partial ablation group ($P < 0.01$).

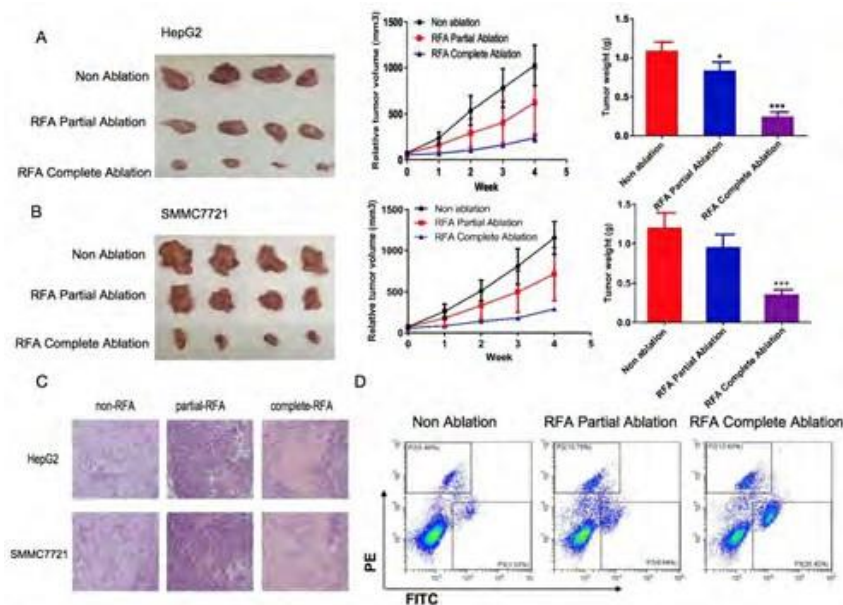


Figure 1: Inhibitory effects of radiofrequency ablation (RFA) on xenotransplant tumor growth in subcutaneous xenograft nude mice. HepG2 and SMMC-7721 cell-derived xenograft nude mice were used to examine the effects of RFA on tumor growth, and the mean tumor sizes and weights were analyzed in the following three groups: No ablation as a control (Nonablation), RFA partial ablation, and RFA complete ablation. (A) HepG2 cell-derived xenograft nude mice. Four weeks after RFA partial or complete ablation, the tumor growth was significantly suppressed as indicated by the smaller tumor size and lower tumor weight compared with the control mice without RFA treatment. (B) SMMC-7721 cell-derived xenograft nude mice. Four weeks after RFA complete ablation, the tumor growth was significantly suppressed as indicated by the smaller tumor size and lower tumor weight compared with the control mice without RFA treatment. (C) Histological findings of tumor sections from HepG2 and SMMC-7721 cell-derived xenograft nude mice. Hematoxylin and eosin staining of the tumor sections revealed a significant reduction in the number of tumor cells in the HepG2 and SMMC-7721 cell-derived xenograft nude mice treated with complete or partial RFA ablation compared with the control mice. (D) Flow cytometry analysis of pyroptotic cells in subcutaneous xenograft nude mice treated with complete or partial RFA ablation in comparison with the control mice. Data are presented as the mean \pm SD, and $P < 0.05$ indicated a significant difference between groups. * $P < 0.05$; *** $P < 0.001$.

RFA Induced Pyroptosis in Subcutaneous Xenograft Nude Mice

Given the inhibitory effects of RFA on tumor growth, we next assessed pyroptosis in subcutaneous xenograft nude mice at different time points after RFA treatment. Immunohistochemistry and western blot analysis were performed to examine the key proteins involved in the inflammation and in pyroptosis in the liver tissues from the HepG2 and SMMC-7721 cell-derived xenograft nude mice. The immunohistochemistry results showed that the protein levels of AIM2, NLRP3, and caspase-1 were significantly greater in the liver tissue sections from the HepG2 and SMMC-7721 cell-derived xenograft nude mice treated with RFA partial or complete ablation, compared with those in the control group ($P < 0.05$) (Figure 2A–B). In addition, a greater effect of RFA on the protein expression of AIM2, NLRP3, and caspase-1 was observed in the HepG2 and SMMC-7721 cell-derived xenograft nude mice treated

with RFA complete ablation in comparison with partial ablation (Figure 2A–B). Western blot analysis revealed similar findings to the immunohistochemistry results. Additionally, the mRNA and protein levels of γ -H2AX and DNA-PK were significantly greater in the HepG2 and SMMC-7721 cell-derived xenograft nude mice treated with RFA partial or complete ablation versus no RFA ablation ($P < 0.05$) (Figure 2C–F), and a greater effect was found in the RFA complete ablation group versus the partial ablation group (Figure 2C–F).

The mean levels of serum IL-1 β and IL-18 were significantly greater in the HepG2 and SMMC-7721 cell-derived xenograft nude mice treated with RFA partial or complete ablation after four weeks of treatment ($P < 0.05$) (Figs. 3A–B). Notably, there was a greater effect of RFA on the serum levels of IL-1 β and IL-18 in the HepG2 and SMMC-7721 cell-derived xenograft nude mice treated with RFA complete ablation in comparison with those treated with partial ablation (Figure 3).

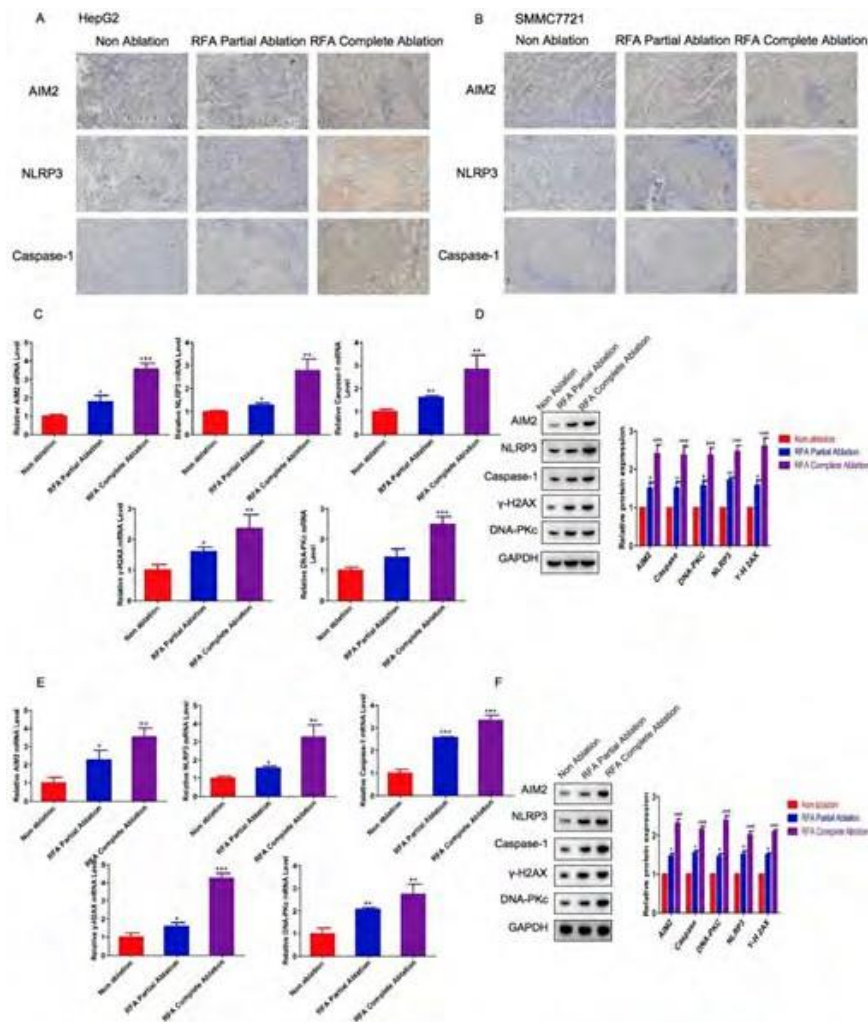


Figure 2: The levels of inflammasome- and pyroptosis-related molecules before and after radiofrequency ablation (RFA) in subcutaneous xenograft nude mice. HepG2 and SMMC-7721 cell-derived xenograft nude mice were treated with RFA partial ablation, RFA complete ablation, or no ablation as a control (Nonablation). After 4 weeks, the liver tissues were collected for subsequent analysis. Immunohistochemical analysis of inflammasome proteins before and after RFA in (A) HepG2 cell-derived xenograft nude mice and (B) SMMC-7721 cell-derived xenograft nude mice. Hepatic AIM2, NLRP3, caspase-1, γ -H2AX, and DNA-PKc (C) mRNA and (D) protein expression levels in HepG2 cell-derived xenograft nude mice. Hepatic AIM2, NLRP3, caspase-1, γ -H2AX, and DNA-PKc (E) mRNA and (F) protein expression levels in SMMC-7721 cell-derived xenograft nude mice. The hepatic AIM2, NLRP3, caspase-1, γ -H2AX, and DNA-PKc mRNA and protein expression levels were significantly greater in the HepG2 and SMMC-7721 cell-derived xenograft nude mice treated with RFA partial or complete ablation versus no RFA ablation, and there were greater effects on these protein levels in the RFA complete ablation group versus the partial ablation group. Data are expressed as the mean \pm SD. $P < 0.05$ indicated as significant difference between groups. * $P < 0.05$; ** $P < 0.01$; *** $P < 0.001$.

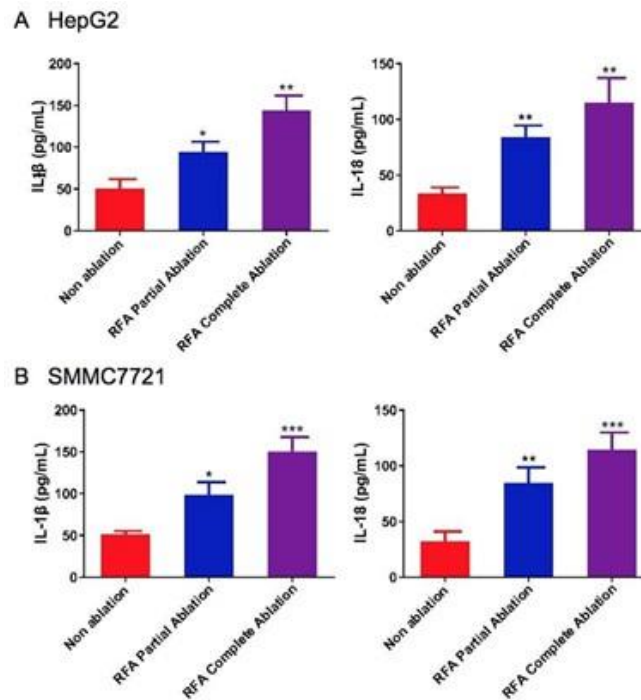


Figure 3: Serum levels of IL-1 β and IL-18 before and after radiofrequency ablation (RFA) in subcutaneous xenograft nude mice. These serum levels of IL-1 β and IL-18 were examined by ELISA in (A) HepG2 cell-derived xenograft nude mice and (B) SMMC-7721 cell-derived xenograft nude mice after 4 weeks of RFA partial ablation, RFA complete ablation, or no ablation. Data are expressed as the mean \pm SD. $P < 0.05$ indicated as significant difference between groups. * $P < 0.05$; ** $P < 0.01$; *** $P < 0.001$.

AIM2 Exerted a Role in RFA-Induced Pyroptosis in Hepatoma Cells

Intrigued by the animal study findings, we further investigated the biological role of AIM2 in RFA-induced pyroptosis in hepatoma SMMC-7721 cells. A cell proliferation assay revealed that down-regulation of AIM2 enhanced the proliferation of SMMC-7721 cells in a time-dependent manner (Figure 4A); by contrast, overexpression of AIM2 attenuated the proliferation of SMMC-7721 cells in a time-dependent manner (Figure 4B). In addition, exposure to RFA resulted in a marked increase in LDH release in comparison with no RFA treatment. Furthermore, overexpression of AIM2 with Lv-AIM2 enhanced the LDH release compared with the control SMMC-7721 cells (Figure 4C).

Pyroptosis is a form of programmed cell death that can affect tumor cell proliferation. Therefore, we examined the effects of RFA on pyroptosis in hepatoma SMMC-7721 cells with overexpression or silencing of AIM2. Flow cytometry assays showed that RFA induced pyroptosis compared with no RFA (Fig. 5A). Additionally, overexpression of AIM2 with Lv-AIM2 enhanced pyroptosis, whereas silencing of AIM2 with shAIM2 diminished pyroptosis in SMMC-7721 cells (Figure 5A).

qRT-PCR revealed that the hepatic γ -H2AX and DNA-PKc mRNA levels were significantly greater in the SMMC-7721 cell treat-

ed with RFA versus those not treated with RFA. Moreover, overexpression of AIM2 increased hepatic γ -H2AX and DNA-PKc mRNA expression, while silencing of AIM2 led to a decrease in the hepatic γ -H2AX and DNA-PKc mRNA levels in the SMMC-7721 cells (Figure 5B). Similarly, the western blot results showed that the hepatic γ -H2AX, DNA-PKc, and caspase-1 levels were significantly greater in the SMMC-7721 cells treated with RFA versus those not treated with RFA and that overexpression of AIM2 increased hepatic γ -H2AX and DNA-PKc protein expression; by contrast, silencing of AIM2 suppressed the hepatic γ -H2AX and DNA-PKc protein levels in SMMC-7721 cells (Figure 5C).

Furthermore, RFA treatment caused increases in hepatic IL-1 β and IL-18 mRNA expression in SMMC-7721 cells as well as protein expression in the cell culture supernatant (Figure 6). Notably, SMMC-7721 cells with overexpression of AIM2 exhibited dramatic increases in both hepatic IL-1 β and IL-18 mRNA expression as well as protein expression in the cell culture supernatant. In contrast, silencing of AIM2 in SMMC-7721 cells inhibited both hepatic IL-1 β and IL-18 mRNA expression as well as protein expression in the cell culture supernatant (Figure 6). Consistent with the changes in hepatic IL-1 β and IL-18 mRNA expression, the protein levels in the cell culture supernatant were also altered. These results were in agreement with AIM2 exerting a biological role in RFA-induced pyroptosis in HCC.

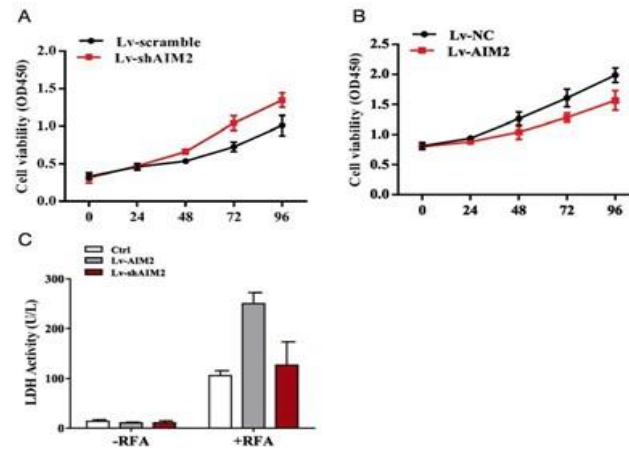


Figure 4: Effects of silencing or overexpression of AIM2 on the proliferation of SMMC-7721 cells and LDH release. A proliferation assay showed the effects of (A) silencing or (B) overexpression of AIM2 on the cell viability of SMMC-7721 cells. Silencing of AIM2 with AIM2-specific shRNA (shAIM) enhanced the proliferation of SMMC-7721 cells compared with the scrambled shRNA control. By contrast, overexpression of AIM2 with Lv-AIM attenuated the proliferation of SMMC-7721 cells in comparison with the nonspecific control (NC). A lactate dehydrogenase (LDH) release assay revealed (C) the effects of silencing or overexpression of AIM2 on the supernatant LDH activity with or without exposure to RFA. Data are expressed as the mean \pm SD. $P < 0.05$ indicated a significant difference between groups.

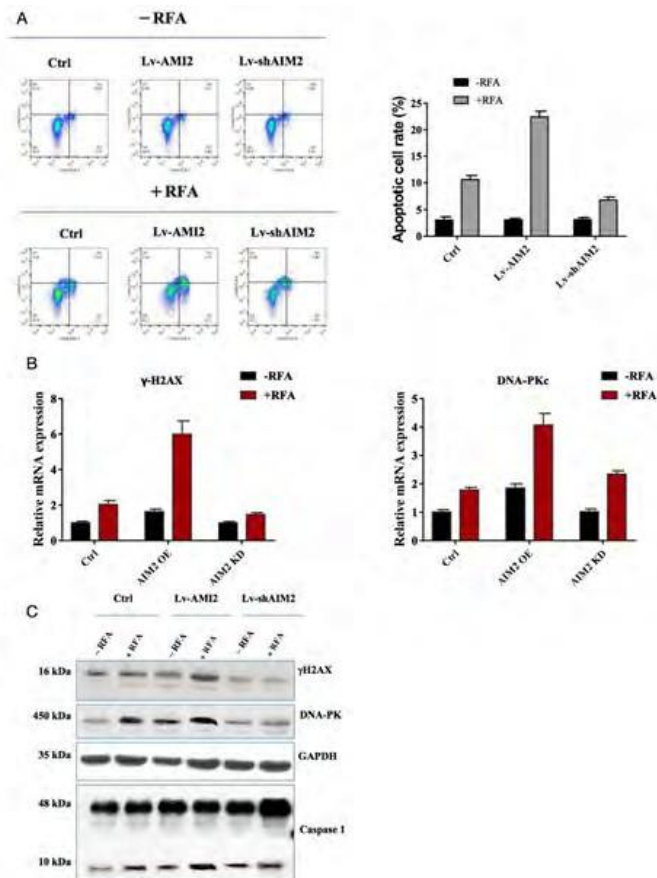


Figure 5: Effects of overexpression and silencing of AIM2 on radiofrequency ablation (RFA)-induced pyroptosis and pyroptosis-related molecules in SMMC-7721 cells. (A) Effects of overexpression and silencing of AIM2 on radiofrequency ablation (RFA)-induced pyroptosis. Pyroptosis was determined by flow cytometry. Overexpression of AIM2 with Lv-AIM induced the pyroptosis of SMMC-7721 cells in comparison with the nonspecific control (NC). By contrast, silencing of AIM2 with AIM2-specific shRNA (shAIM) inhibited the pyroptosis of SMMC-7721 cells compared with the scrambled shRNA control. (B) RT-PCR analysis of the effects of overexpression and knockout of AIM2 on the mRNA levels of pyroptosis-related molecules before and after RFA in SMMC-7721 cells. (C) Western blot analysis of the effects of overexpression and knockout of AIM2 on the protein levels of pyroptosis-related molecules before and after RFA in SMMC-7721 cells.

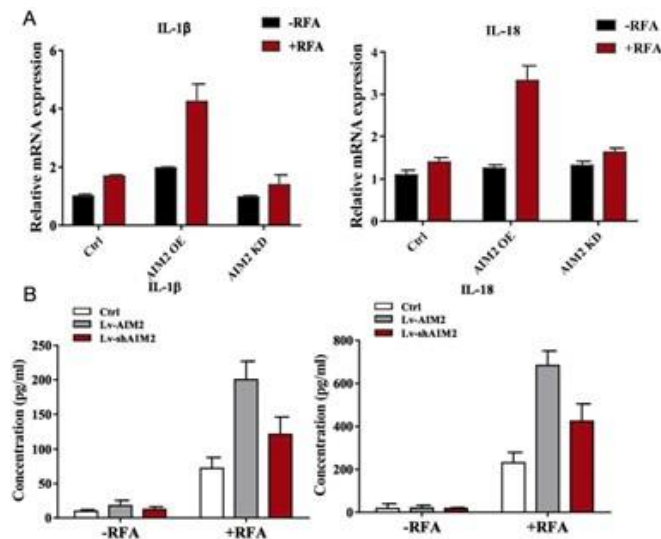


Figure 6: Effects of overexpression and silencing of AIM2 on the cytokine levels in SMMC-7721 cells and in the cell culture supernatant. qRT-PCR analysis was conducted to measure the mRNA expression levels of IL-1 β and IL-18, and ELISA was performed to determine the serum levels of IL-1 β and IL-18 in the cell culture supernatant of SMMC-7721 cells. (A) The effects of overexpression of AIM2 with Lv-AIM2 on the cytokine levels in SMMC-7721 cells and in the cell culture supernatant. (B) The effects of silencing of AIM2 with Lv-shAIM2 on the cytokine levels in SMMC-7721 cells and in the cell culture supernatant.

5. Discussion

The major novel findings of this study are summarized as follows: [1] RFA treatment significantly inhibited tumor growth in BALB/c nude mice bearing HepG2 or SMMC-7721 cell-derived xenografts compared with the controls not receiving RFA (Figure 1). [2] RFA induced pyroptotic cell death of HepG2 or SMMC-7721 cells in the xenograft nude mice, as evidenced by the fact that the levels of AIM2, NLRP3, caspase-1, γ -H2AX, and DNA-PK in the liver tissues were significantly elevated in the mice treated with RFA versus those of the controls (Figure 2); these serum levels of IL-1 β and IL-18 were significantly greater in the HepG2 or SMMC-7721 cell-derived xenograft mice treated with RFA compared to those not receiving RFA (Figure 3); and greater effects were observed in the RFA complete ablation group versus the partial ablation group of xenograft nude mice (Figure 2–3). (3) Functional and mechanistic studies performed *in vitro* indicated that AIM2 exerted a direct role in RFA-induced pyroptosis; these findings were supported by studies using knockout or overexpression of AIM2 (Figure 4–6). These results suggest that RFA suppresses the inhibitory effect of RFA on the proliferation of hepatoma cells involved in the induction of pyroptosis through AIM2-inflammasome signaling. It has been well documented that hepatic inflammation represents a key event in the development of HCC [6]. The last decade has witnessed rapid progress in the understanding of activation of the inflammasome in the pathogenesis of HCC. For instance, it has been found that AIM2-like receptors are capable of inducing the activation of inflammasomes and thereby further activating caspases. Once activated, caspases can mediate the generation, maturation, and secretion of proinflammatory cytokines, mainly IL-1 β

and IL-18. As a result, excessive secretion of these inflammatory cytokines (e.g., IL-1 β and IL-18) ultimately causes a form of cell death, referred to as pyroptosis [15–17]. HBV and HCV infections are well-known causes of HCC. In fact, nearly 90% of HCC cases are associated with chronic hepatic inflammation, for which HCC is a good example of inflammation-related cancer [18, 19]. Therefore, inflammasome-associated molecular mechanisms have been a major focus in HCC research. In the present study, we found that RFA treatment induced cell death in the form of pyroptosis in nude mice bearing HepG2 or SMMC-7721 cell-derived xenografts as well as in hepatoma cells. Our findings further supported that the AIM2-activated inflammasome activated caspase-1, through which it enhanced the formation and secretion of inflammatory cytokines (IL-1 β and IL-18) and resulted in pyroptosis.

Numerous previous studies have shown that the hepatic AIM2 levels are significantly reduced in HCC samples compared with matched histologically normal tissues from the same patients and that a lower AIM2 expression is significantly correlated with more advanced HCC [20–22]. In addition, it has been found that lower AIM2 levels are significantly correlated with more advanced HCC, poorer tumor differentiation, and greater invasion and metastasis abilities, suggesting that the loss of AIM2 may contribute to the progression of HCC [20, 21]. Moreover, Ma et al. have shown that the overexpression of AIM2 significantly suppressed the tumor growth in a xenograft mouse model [20]. Furthermore, the potential role of AIM2 in the development of HCC has been recently investigated, and the results demonstrate that genetic silencing of AIM2 or caspase-1/11 protects mice against the occurrence of HCC [23, 24]. Our findings are consistent with these previous

studies. To date, the exact roles of AIM2 and AIM2-activated inflammasomes in the action of RFA treatment for HCC have not been explored. Our results indicate that the inhibitory effects of RFA on the proliferation of hepatoma cells may involve the induction of pyroptosis through AIM2-inflammasome signaling. We postulated that exposure to RFA can cause cellular damage, triggering the release of self-DNA, which can also be sensed by AIM2 and thereby lead to the assembly and activation of the inflammasome complex in response to RFA but in the absence of infection.

Our study may have some potential limitations. For instance, we found that AIM2 was markedly elevated in response to RFA in the mice bearing HepG2 or SMMC-7721 cell-derived xenografts as well as in cell cultures, but the molecular pathways through which AIM2 is upregulated remain unknown. We propose that, in the absence of infection caused by pathogens, AIM2 may sense RFA-associated DNA, assemble, activate the inflammasome complex, and promote secretion of inflammatory cytokines, thus inducing pyroptosis. Given that compelling evidence of the actions of AIM2 beyond the inflammasome complex has been reported [25-30], it would be interesting to explore whether AIM2 can play an inflammasome-independent role in HCC and RFA treatment for HCC. Further in-depth investigations on the underlying molecular mechanisms are currently underway in our laboratory.

6. Conclusions

Taken together, we found that RFA suppressed tumor growth, and, more notably, RFA treatment induced pyroptosis in HCC. In addition, AIM2-mediated activation of inflammasome signaling was identified as an important cell death mechanism. Therefore, these findings advance our understanding of the biological function of AIM2, and intervention of AIM2-mediated inflammasome signaling may assist in improving RFA treatment for HCC.

References

1. Yang JD, Hainaut P, Gores GJ, Amadou A, Plymoth A, Roberts LR. A global view of hepatocellular carcinoma: trends, risk, prevention and management. *Nat Rev Gastroenterol Hepatol.* 2019; 16: 589-604.
2. Llovet JM, Kelley RK, Villanueva A, Singal AG, Pikarsky E, Roayaie S, et al. Hepatocellular carcinoma. *Nat Rev Dis Primers.* 2021; 7:6.
3. Chen W, Zheng R, Baade PD, Zhang S, Zeng H, Bray F, et al. Cancer statistics in China. *CA Cancer J Clin.* 2016; 66: 115-132.
4. Akinyemiju T, Abera S, Ahmed M, Alam N, Alemayohu MA, Allen C, et al. The burden of primary liver cancer and underlying etiologies from 1990 to 2015 at the global, regional, and national level: Results from the global burden of disease study. *JAMA Oncol.* 2017; 3: 1683-1691.
5. Szabo G, Petrasek J. Inflammasome activation and function in liver disease. *Nat Rev Gastroenterol Hepatol.* 2015; 12: 387-400.
6. Galun E. Liver inflammation and cancer: The role of tissue microenvironment in generating the tumor-promoting niche (TPN) in the development of hepatocellular carcinoma. *Hepatology.* 2016; 63:354-356.
7. Man SM. Inflammasomes in the gastrointestinal tract: infection, cancer and gut microbiota homeostasis. *Nat Rev Gastroenterol Hepatol.* 2018; 15: 721-737.
8. Luan J, Ju D. Inflammasome: A double-edged sword in liver diseases. *Front Immunol.* 2018; 9: 2201.
9. Lugrin J, Martinon F. The AIM2 inflammasome: Sensor of pathogens and cellular perturbations. *Immunol Rev.* 2018; 281: 99-114.
10. Wang B, Yin Q. AIM2 inflammasome activation and regulation: A structural perspective. *J Struct Biol.* 2017; 200: 279-282.
11. Jin T, Perry A, Jiang J, Smith P, Curry JA, Unterholzner L, et al. Structures of the HIN domain: DNA complexes reveal ligand binding and activation mechanisms of the AIM2 inflammasome and IFI16 receptor. *Immunity.* 2012; 36: 561-571.
12. Morrone SR, Matyszewski M, Yu X, Delannoy M, Egelman E, Sohn J. Assembly-driven activation of the AIM2 foreign-dsDNA sensor provides a polymerization template for downstream ASC. *Nat Commun.* 2015; 6: 7827.
13. Fernandes-Alnemri T, Yu JW, Datta P, Wu J, Alnemri ES. AIM2 activates the inflammasome and cell death in response to cytoplasmic DNA. *Nature.* 2009; 458: 509-513.
14. Hornung V, Ablasser A, Charrel-Dennis M, Bauernfeind F, Horvath G, Caffrey DR, et al. AIM2 recognizes cytosolic dsDNA and forms a caspase-1-activating inflammasome with ASC. *Nature.* 2009; 458: 514-518.
15. Martinon F, Burns K, Tschopp J. The inflammasome: a molecular platform triggering activation of inflammatory caspases and processing of proIL-beta. *Mol Cell.* 2002; 10: 417-426.
16. Kayagaki N, Wong MT, Stowe IB, Ramani SR, Gonzalez LC, Akashi-Takamura S, et al. Noncanonical inflammasome activation by intracellular LPS independent of TLR4. *Science.* 2013; 341: 1246-1249.
17. Liu X, Zhang Z, Ruan J, Pan Y, Magupalli VG, Wu H, et al. Inflammasome-activated gasdermin D causes pyroptosis by forming membrane pores. *Nature.* 2016; 535: 153-158.
18. Llovet JM, Zucman-Rossi J, Pikarsky E, Sangro B, Schwartz M, Sherman M, et al. Hepatocellular carcinoma. *Nat Rev Dis Primers.* 2016; 2: 16018.
19. Ringelhan M, Pfister D, O'Connor T, Pikarsky E, Heikenwalder M. The immunology of hepatocellular carcinoma. *Nat Immunol.* 2018; 19: 222-232.
20. Ma X, Guo P, Qiu Y, Mu K, Zhu L, Zhao W, et al. Loss of AIM2 expression promotes hepatocarcinoma progression through activation of mTOR-S6K1 pathway. *Oncotarget.* 2016; 7: 36185-36197.
21. Chen SL, Liu LL, Lu SX, Luo RZ, Wang CH, Wang H, et al. HBx-mediated decrease of AIM2 contributes to hepatocellular carcinoma metastasis. *Mol Oncol.* 2017; 11: 1225-1240.
22. Sonohara F, Inokawa Y, Kanda M, Nishikawa Y, Yamada S, Fujii T, et al. Association of Inflammasome Components in Background Liver with Poor Prognosis After Curatively-resected Hepatocellular Carcinoma. *Anticancer Res.* 2017; 37: 293-300.

- gaba-Chueca F, Gómez-Hurtado I, et al. AIM2 deficiency reduces the development of hepatocellular carcinoma in mice. *Int J Cancer*. 2018; 143: 2997-3007.
24. Macek Jilkova Z, Kurma K, Decaens T. Animal models of hepatocellular carcinoma: The role of immune system and tumor microenvironment. *Cancers (Basel)*. 2019; 11: 1478.
25. El-Zaatari M, Bishu S, Zhang M, Grasberger H, Hou G, Haley H, et al. Aim2-mediated/IFN- β -independent regulation of gastric metaplastic lesions via CD8+ T cells. *JCI Insight*. 2020; 5: e94035.
26. Furrer A, Hottiger MO, Valaperti A. Absence in Melanoma2 (AIM2) limits pro-inflammatory cytokine transcription in cardiomyocytes by inhibiting STAT1 phosphorylation. *Mol Immunol*. 2016; 74: 47-58.
27. Farshchian M, Nissinen L, Siljamäki E, Riihilä P, Piipponen M, Kivisaari A, et al. Tumor cell-specific AIM2 regulates growth and invasion of cutaneous squamous cell carcinoma. *Oncotarget*. 2017; 8: 45825-45836.
28. Man SM, Zhu Q, Zhu L, Liu Z, Karki R, Malik A, et al. Critical Role for the DNA Sensor AIM2 in Stem Cell Proliferation and Cancer. *Cell*. 2015; 162: 45-58.
29. Wilson JE, Petrucelli AS, Chen L, Koblansky AA, Truax AD, Oyama Y, et al. Inflammasome-independent role of AIM2 in suppressing colonic tumorigenesis via DNA-PK and Akt. *Nat Med*. 2015; 21: 906-913.
30. Qi M, Dai D, Liu J, Li Z, Liang P, Wang Y, et al. AIM2 promotes the development of non-small cell lung cancer by modulating mitochondrial dynamics. *Oncogene*. 2020; 39: 2707-2723.